The crystal truncation rod scattering of neutrons and the multiwave dynamical theory of diffraction

1999 J. Phys.: Condens. Matter 11 5767

(http://iopscience.iop.org/0953-8984/11/30/308)

J. Phys.: Condens. Matter **11** (1999) 5767–5779. Printed in the UK PII: S0953-8984(99)98519-3

The crystal truncation rod scattering of neutrons and the multiwave dynamical theory of diffraction

O Litzman† and P Mikulík‡

† Department of Theoretical Physics and Astrophysics, Faculty of Science, Masaryk University, Kotlářská 2, 611 37 Brno, Czech Republic

‡ Laboratory of Thin Films and Nanostructures, Faculty of Science, Masaryk University, Kotlářská 2, 611 37 Brno, Czech Republic

Received 20 October 1998, in final form 26 April 1999

Abstract. The influence of the Bragg diffractions on the coplanar and non-coplanar crystal truncation rod scattering is studied using the Ewald multiwave dynamical theory of diffraction. The resulting formulae are compared with the approximate ones of the kinematical theory and geometrical optics approximations.

1. Introduction

The crystal surface lowers the three-dimensional translational symmetry of an ideal infinite crystal given by the basic lattice vectors $(\boldsymbol{a}_1, \boldsymbol{a}_2, \boldsymbol{a}_3)$ into a two-dimensional one, given by the translational vectors $(\boldsymbol{a}_1, \boldsymbol{a}_2)$. The vectors $\boldsymbol{a}_1, \boldsymbol{a}_2$ are assumed to lie in the bordering surfaces of the crystalline layer. We denote by $\boldsymbol{k} = \boldsymbol{k}^{\parallel} + \boldsymbol{k}^{\perp}$ the wave vector of the incident wave

$$f = A\mathrm{e}^{\mathrm{i}\boldsymbol{k}\cdot\boldsymbol{r}} \tag{1.1}$$

and by $(\boldsymbol{b}_1, \boldsymbol{b}_2)$ the basic vectors of the lattice reciprocal to $(\boldsymbol{a}_1, \boldsymbol{a}_2)$, and also by $\boldsymbol{e}_3$ the unit vector in the direction of the inner normal; see figure 1. Then the wave vectors of the waves transmitted $(\boldsymbol{K}^{+}_{pq}(\boldsymbol{k}))$ and reflected $(\boldsymbol{K}^{-}_{pq}(\boldsymbol{k}))$ by a crystalline layer are

$$\begin{aligned} \boldsymbol{K}^{\pm}_{pq}(\boldsymbol{k}) &= \boldsymbol{k}^{\parallel} + p\boldsymbol{b}_1 + q\boldsymbol{b}_2 \pm \boldsymbol{e}_3 K_{pqz}(\boldsymbol{k}) \\ K_{pqz}(\boldsymbol{k}) &= +\sqrt{k^2 - |\boldsymbol{k}^{\parallel} + p\boldsymbol{b}_1 + q\boldsymbol{b}_2|^2} \end{aligned} \tag{1.2}$$

with p, q integers. Obviously, there are a finite number of reflected waves with real $K_{pqz}(\boldsymbol{k})$ and an infinite number of non-radiative waves with pure imaginary $K_{pqz}(\boldsymbol{k})$ (*evanescent waves*).

It has been found that, to study the geometry of the scattering, the 'Γ^{-}_{pq}-diagrams' [1] can be used to advantage. We define the quantities

$$\theta^{\pm}_{pq}(\boldsymbol{k}) = \boldsymbol{a}_3 \cdot \boldsymbol{K}^{\pm}_{pq}(\boldsymbol{k}) \tag{1.3}$$

geometrically representing the projection of $\boldsymbol{K}^{\pm}_{pq}(\boldsymbol{k})$ to $\boldsymbol{a}_3$. The incident wave (1.1) is in the Bragg and/or Laue diffraction position $(pq\ell)$ on a crystal truncation rod, CTR, (pq), if, for its wave vector $\boldsymbol{k} = \boldsymbol{K}^{+}_{00}$ (see formula (2.9) in [1]),

$$\theta^{+}_{00}(\boldsymbol{k}) = \theta^{\mp}_{pq}(\boldsymbol{k}) + 2\pi\ell \qquad \text{with } \ell \text{ integer} \tag{1.4}$$

holds, the diffraction vector being $p\boldsymbol{g}_1 + q\boldsymbol{g}_2 - \ell\boldsymbol{g}_3$. Here $(\boldsymbol{g}_1, \boldsymbol{g}_2, \boldsymbol{g}_3)$ are the basic vectors of the lattice reciprocal to $(\boldsymbol{a}_1, \boldsymbol{a}_2, \boldsymbol{a}_3)$. We introduce

$$\Gamma^{\mp}_{pq}(\boldsymbol{k}) = \boldsymbol{a}_3 \cdot (\boldsymbol{k} - \boldsymbol{K}^{\mp}_{pq}) = \theta^{+}_{00}(\boldsymbol{k}) - \theta^{\mp}_{pq}(\boldsymbol{k}) \tag{1.5}$$

0953-8984/99/305767+13$30.00

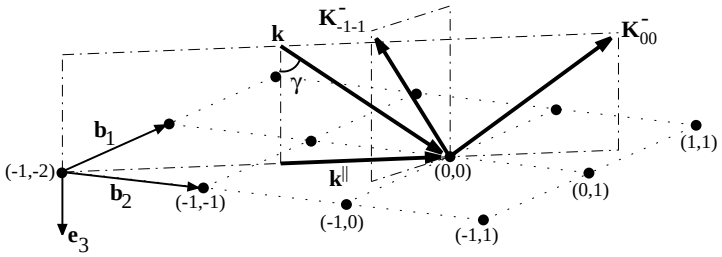

Figure 1. A drawing of the scattering geometry used in the calculations in the following graphs. We assume a semi-infinite crystal with a bcc lattice with $\boldsymbol{a}_1 = a(1,0,0)$, $\boldsymbol{a}_2 = a(0,1,0)$, $\boldsymbol{a}_3 = (a/2)(1,1,1)$ and $\boldsymbol{a}_1, \boldsymbol{a}_2$ lying in the crystal surface plane. This defines the two-dimensional reciprocal lattice of $(\boldsymbol{b}_1, \boldsymbol{b}_2)$; $\boldsymbol{b}_1 \parallel \boldsymbol{a}_1$, $\boldsymbol{b}_2 \parallel \boldsymbol{a}_2$, $b_1 = b_2 = 2\pi/a$. We choose the tangential component $\boldsymbol{k}^{\parallel}$ of the incident wave vector ($\lambda/a = 0.725$) as parallel to the direction $\boldsymbol{a}_1 + 2\boldsymbol{a}_2 \parallel \boldsymbol{b}_1 + 2\boldsymbol{b}_2$.

where $(\boldsymbol{K}^{\mp}_{pq} - \boldsymbol{k})$ is the scattering wave vector in a vacuum. Then the diffraction conditions can be written as

$$\Gamma^{\pm}_{pq}(\boldsymbol{k}) = 2\pi\ell \tag{1.6}$$

where the + sign means the Laue case and − the Bragg case. This condition coincides with the third Laue diffraction condition written in the usual notation [2]: $\frac{1}{2}(\boldsymbol{K}_{pq\ell} - \boldsymbol{k}) \cdot \boldsymbol{a}_3 = \ell\pi$. In most experiments the plane of incidence and the wavelength are kept constant and only the angle of incidence γ (measured from the inner normal to the surface) varies; $\boldsymbol{k} = \boldsymbol{k}(\gamma)$. Then the positions of the Bragg angles $\gamma^{\mathrm{B}}_{pq\ell}$ follow directly from (1.6).

Let us demonstrate the meaning of (1.3)–(1.6) for the scattering geometry defined in figure 1: a bcc lattice with the surface plane $(\boldsymbol{a}_1, \boldsymbol{a}_2)$; the tangential component of the incident wave $\boldsymbol{k}$ is parallel to the direction $\boldsymbol{a}_1 + 2\boldsymbol{a}_2 \parallel \boldsymbol{b}_1 + 2\boldsymbol{b}_2$. The incident wave $\boldsymbol{k} \equiv \boldsymbol{K}^{+}_{00}$ excites (among others) the specularly reflected wave $\boldsymbol{K}^{-}_{00} = \boldsymbol{k}^{\parallel} - \boldsymbol{k}^{\perp}$ and the non-coplanar reflected wave

$$\boldsymbol{K}^{-}_{-1-1} = \boldsymbol{k}^{\parallel} - \boldsymbol{b}_1 - \boldsymbol{b}_2 - \boldsymbol{e}_3\sqrt{k^2 - |\boldsymbol{k}^{\parallel} - \boldsymbol{b}_1 - \boldsymbol{b}_2|^2}.$$

All of the vectors $\boldsymbol{k}$, $\boldsymbol{K}^{-}_{00}$, $\boldsymbol{K}^{-}_{-1-1}$ depend on the angle of incidence γ. For most angles of incidence the wave fields of $\boldsymbol{K}^{-}_{00}$ and $\boldsymbol{K}^{-}_{-1-1}$ are 'weak'. But if $\boldsymbol{a}_3 \cdot (\boldsymbol{k} - \boldsymbol{K}_{-1-1}) = 2\pi\ell$ (which means that $\Gamma^{-}_{-1-1} = \theta^{+}_{00}(\boldsymbol{k}) - \theta^{-}_{-1-1}(\boldsymbol{k}) = 2\pi\ell$; see (1.4)), then the incident wave $\boldsymbol{k}$ fulfils the Bragg diffraction condition for CTR $(-1\,-1)$ and the wave $\boldsymbol{K}^{-}_{-1-1}$ is strong.

In figure 2 the Γ^{-}_{pq}-diagrams are employed to demonstrate the reflection on a bcc lattice with the scattering geometry as in figure 1. From the diagram it follows that for the positive angles of incidence $\gamma \in (0, 90^{\circ})$ two coplanar reflections $(0,0)$, $(-1,-2)$ and seven non-coplanar reflections $(0,1)$, $(1,0)$, $(1,-1)$, $(-1,-1)$, $(0,-2)$, $(0,-1)$, $(-1,0)$ exist. All other excited waves are evanescent. The inset figure demonstrates the detail close to the Bragg angle γ^{B}, where the total reflection occurs in the region of $(\gamma^{\mathrm{f}}, \gamma^{\mathrm{i}})$.

Let us for example consider the intensities of the reflected beams in the directions $\boldsymbol{K}^{-}_{00}(\boldsymbol{k})$ (*specular reflection*) and $\boldsymbol{K}_{-1-1}(\boldsymbol{k})$ (*non-coplanar reflection*) in the gamma-diagrams Γ^{-}_{00} and Γ^{-}_{-1-1} in figure 2. The regions of total reflections in these directions are near the angles of incidence $\gamma^{\mathrm{B}}_{001}$ and $\gamma^{\mathrm{B1}}_{-1-12}, \gamma^{\mathrm{B2}}_{-1-12}$, respectively. It is clear that the total reflection of the specularly reflected beam at the angle of incidence $\gamma^{\mathrm{B}}_{001}$ must influence the reflectivity in the direction $\boldsymbol{K}^{-}_{-1-1}$ between the angles of incidence $\gamma^{\mathrm{B1}}_{-1-12}$ and $\gamma^{\mathrm{B2}}_{-1-12}$, i.e. the crystal truncation rod scattering between the two regions of the total reflection in the direction $\boldsymbol{K}^{-}_{-1-1}$. Thus for

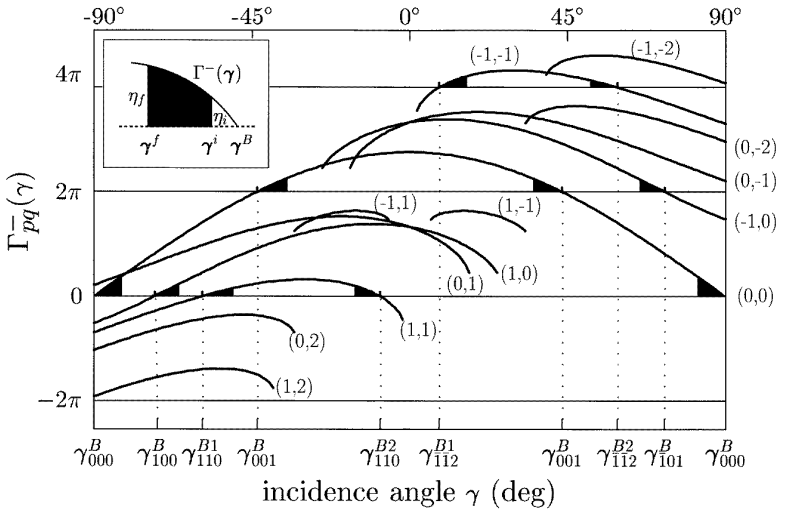

Figure 2. Gamma-diagrams $\Gamma^-_{pq}(\gamma) = \theta^+_{00} - \theta^-_{pq}$ for the sample and scattering geometry described in figure 1. The angles $\gamma^{\mathrm{B}}_{pq\ell}$ are the angles of incidence (measured from the inner normal) for which the Bragg diffraction conditions $\Gamma^-_{pq}(\gamma^{\mathrm{B}}_{pq\ell}) = 2\pi\ell$ are satisfied. The inset figure demonstrates the distance $\eta_{pq\ell} = \Gamma^-_{pq}(\gamma) - 2\pi\ell \geqslant 0$ determining the position (which is close to $\gamma^{\mathrm{B}}_{pq\ell}$) and the width $(\gamma^{\mathrm{i}}_{pq\ell} - \gamma^{\mathrm{f}}_{pq\ell})$ of the Darwin plateau for $Q_0 > 0$. For $Q_0 < 0$ the Darwin plateaus are in the regions $\eta_{pq\ell} \leqslant 0$. In the main figure the scale of the shaded Darwin plateaus could not be preserved.

the study of the CTR scattering the two-beam approximation is not adequate, and a many-beam treatment is required.

The conventional dynamical theory of diffraction addresses the reflectivity of the crystal near the Bragg peaks, studying the well-known rocking curves [2–4]. Recently, the interest in the intensity far from the Bragg peaks, i.e. the CTR scattering, has been motivated by the fact that this region is more sensitive to the defects of the ideal crystal surface than the regions of the rocking curves. The CTR scattering was studied by many authors by means of both the kinematical [5–7] and the dynamical theories of diffraction, using the Laue [8, 9] or Darwin [10, 11] method.

The difficulty in computing the reflectivity far from the Bragg reflection position consists in the fact that the Ewald sphere intersecting the origin of the reciprocal space is not close to any other node of the reciprocal lattice. Thus the usual two-beam approximation is not adequate; all waves corresponding to all CTRs, or at least all waves corresponding to the nodes 'near' the Ewald sphere, should be considered. In other words, the CTR scattering should be handled within the multiwave theory. But using the standard Bethe–Laue formulation of diffraction [2, 3], the contribution to the reflectivity of the individual solutions of the dispersion relation is not clear.

The use of the mathematical formalism for Ewald's dynamical theory of diffraction has provided another approach to this problem. In the original version of Ewald's theory [12, 13] the crystal was realized as a system of Hertz dipoles, situated at the crystal lattice points and coupled via retarded electromagnetic forces, which are brought into forced vibrations by the external electromagnetic wave. This model of the crystal is of course far from physical reality. But Ewald's idea can be used for the interaction of particles with point diffraction centres such

as the interaction of neutrons with a crystal [1, 4, 14–17]. The dispersion relation, giving the z-components κ_z of the wave vectors of the refracted waves in this theory, reads (see equation (2.18a) in [1])

$$1 + QS'(\boldsymbol{k}) + \frac{2\pi \mathrm{i} Q}{|\boldsymbol{a}_1 \times \boldsymbol{a}_2|} \sum_{pq} \frac{1}{K_{pqz}} \left[\frac{\mathrm{e}^{\mathrm{i}\theta^+_{pq}}}{\mathrm{e}^{\mathrm{i}\psi} - \mathrm{e}^{\mathrm{i}\theta^+_{pq}}} + \frac{\mathrm{e}^{-\mathrm{i}\theta^-_{pq}}}{\mathrm{e}^{-\mathrm{i}\psi} - \mathrm{e}^{-\mathrm{i}\theta^-_{pq}}} \right] = 0 \qquad (1.7)$$

where $\psi = a_{3z}\kappa_z$ and $Q = Q_0/(1 + \mathrm{i}kQ_0)$ is the neutron scattering length. The plane lattice sum $S'(\boldsymbol{k})$ (see equation (16) in [15]) is of the order of $1/a$. Thus the intensity of the reflected waves in this formalism is given not by the distance of the reciprocal-lattice nodes from the Ewald sphere, but by the relative positions of the poles $\theta^{\pm}_{pq}(\boldsymbol{k})$ of the dispersion relation (1.7).

This paper is structured as follows. In section 2 we introduce the algebraic formalism for the study of the CTR scattering within the multiwave dynamical theory of diffraction whereby we confine ourselves to a semi-infinite crystal where the formulae can be given in a simple algebraic form. In section 3 we study the influence of the Bragg reflections on the intensity profile of other reflections. In section 4 we compare the results from the dynamical theory of diffraction with those from the kinematical theory and geometrical optics approximations.

2. General formulae for the reflection of neutrons by a semi-infinite crystal in the multiwave theory

Our further considerations are based on the results of our previous papers [1, 15] dealing with the dynamical theory of diffraction of neutrons in Ewald's conception [4, 12, 14].

The reflectivity $\mathcal{R}(\boldsymbol{K}^-_{pq})$ of a semi-infinite crystal in the direction of the wave vector $\boldsymbol{K}^-_{pq}$, equation (1.2), can be computed as follows (see equations (2.15) and (2.16) in [1]):

$$\mathcal{R}(\boldsymbol{K}^-_{pq}) = \left|R_1(\boldsymbol{K}^-_{pq})\right|^2 \left|R_2(\boldsymbol{K}^-_{pq})\right|^2 \frac{k_z}{K_{pqz}} \qquad (2.1)$$

where

$$R_1(\boldsymbol{K}^-_{pq}) = \frac{\mathrm{e}^{\mathrm{i}\psi^+_{00}} - \mathrm{e}^{\mathrm{i}\theta^+_{00}}}{\mathrm{e}^{\mathrm{i}\psi^+_{00}} - \mathrm{e}^{\mathrm{i}\theta^-_{pq}}} \qquad (2.2)$$

$$R_2(\boldsymbol{K}^-_{pq}) = \prod_{(uv)\neq(00)}{}' \frac{\mathrm{e}^{\mathrm{i}\psi^+_{uv}} - \mathrm{e}^{\mathrm{i}\theta^+_{00}}}{\mathrm{e}^{\mathrm{i}\psi^+_{uv}} - \mathrm{e}^{\mathrm{i}\theta^-_{pq}}} \frac{\mathrm{e}^{\mathrm{i}\theta^+_{uv}} - \mathrm{e}^{\mathrm{i}\theta^-_{pq}}}{\mathrm{e}^{\mathrm{i}\theta^+_{uv}} - \mathrm{e}^{\mathrm{i}\theta^+_{00}}}. \qquad (2.3)$$

Here, $\psi^{\pm}_{uv}$ is the solution of the dispersion relation (1.7) near the pole $\theta^{\pm}_{uv}$. It holds that

$$\mathrm{e}^{\mathrm{i}\psi^{\pm}_{uv}} = \mathrm{e}^{\mathrm{i}\theta^{\pm}_{uv}}[1 + \mathrm{O}(1/h_0)] \qquad (2.4)$$

excluding the case where $a_{3z}K_{uvz} \ll 1$. The quantity

$$h_0 = \frac{|\boldsymbol{a}_1 \times \boldsymbol{a}_2|}{2\pi a_{3z} Q_0} \qquad (2.5)$$

for the neutron diffraction is of order 10^4.

By using (2.1)–(2.3) the problem of the reflection of neutrons by a semi-infinite crystal is solved exactly for any angle of incidence and any wavelength, i.e. for the CTR scattering as well. To use them we must of course evaluate the solutions ψ^+_{uv} of the dispersion relation (1.7). The numerical evaluation of ψ^+_{uv} was discussed in [1]. In this paper we shall try to find formulae for the reflection suitable to analytical approximations.

Let us consider the expression (2.3) for $R_2(\boldsymbol{K}^-_{pq})$. Due to (2.4) and (2.5) it holds that

$$\frac{\mathrm{e}^{\mathrm{i}\psi^+_{uv}} - \mathrm{e}^{\mathrm{i}\theta^+_{00}}}{\mathrm{e}^{\mathrm{i}\psi^+_{uv}} - \mathrm{e}^{\mathrm{i}\theta^-_{pq}}} \frac{\mathrm{e}^{\mathrm{i}\theta^+_{uv}} - \mathrm{e}^{\mathrm{i}\theta^-_{pq}}}{\mathrm{e}^{\mathrm{i}\theta^+_{uv}} - \mathrm{e}^{\mathrm{i}\theta^+_{00}}} = 1 + \mathrm{O}(1/h_0). \qquad (2.6)$$

Thus

$$R_2(\boldsymbol{K}^-_{pq}) = 1 + \mathrm{O}(1/h_0) \tag{2.7}$$

excluding the cases where $\theta^+_{00}(\boldsymbol{k}) - \theta^+_{uv}(\boldsymbol{k}) = 0$ (modulo 2π), $(uv) \neq (00)$ and $\theta^-_{pq}(\boldsymbol{k}) - \theta^+_{uv}(\boldsymbol{k}) = 0$ (modulo 2π). The first exclusion is the condition for the Laue diffraction (see (1.5)) and it will be discussed later. The second one will not be considered in this paper. Thus we can write

$$\mathcal{R}(\boldsymbol{K}^-_{pq}) = \mathcal{R}_1(\boldsymbol{K}^-_{pq})[1 + \mathrm{O}(1/h_0)] \tag{2.8}$$

$$\mathcal{R}_1(\boldsymbol{K}^-_{pq}) = |R_1(\boldsymbol{K}^-_{pq})|^2 \frac{k_z}{K_{pqz}}. \tag{2.9}$$

Let us now consider the solution of the dispersion relation (1.7). Let us assume that say $\theta^+_{00}(\boldsymbol{k})$ and $\theta^-_{mn}(\boldsymbol{k})$ are two poles of the dispersion relation (1.7) and let us investigate the solutions ψ^+_{00} and ψ^-_{mn} near these poles. For this purpose let us separate in (1.7) the terms corresponding to the poles θ^+_{00} and θ^-_{mn}. In this way we obtain (see (2.18*c*) in [1])

$$b^{\mathrm{o}}_{00}\frac{\mathrm{e}^{\mathrm{i}\theta^+_{00}}}{\mathrm{e}^{\mathrm{i}\psi} - \mathrm{e}^{\mathrm{i}\theta^+_{00}}} + b^{\mathrm{o}}_{mn}\frac{\mathrm{e}^{-\mathrm{i}\theta^-_{mn}}}{\mathrm{e}^{-\mathrm{i}\psi} - \mathrm{e}^{-\mathrm{i}\theta^-_{mn}}} = F_{00,mn}(\psi) \tag{2.10}$$

where

$$b^{\mathrm{o}}_{pq} = \mathrm{i}\beta_{pq} = -\frac{\mathrm{i}}{h_0 a_{3z} K_{pqz}}. \tag{2.11}$$

Equation (2.10) can formally be considered as a second-order algebraic equation for $\mathrm{e}^{\mathrm{i}\psi}$. Then from (2.10) it follows that

$$\mathrm{e}^{\mathrm{i}\psi} = \frac{F_{00,mn}(\psi) + [F_{00,mn}(\psi) + b^{\mathrm{o}}_{00} + b^{\mathrm{o}}_{mn}]\mathrm{e}^{\mathrm{i}(\theta^+_{00} - \theta^-_{mn})} \pm \sqrt{D_{00,mn}(\psi)}}{2[F_{00,mn}(\psi) + b^{\mathrm{o}}_{mn}]\mathrm{e}^{-\mathrm{i}\theta^-_{mn}}} \tag{2.12}$$

where (see also (2.28) in [1])

$$D_{00,mn}(\psi, \boldsymbol{k}) = 4\beta_{00}\beta_{mn}[1 - Y^2_{mn}(\psi, \boldsymbol{k})]\mathrm{e}^{\mathrm{i}(\theta^+_{00} - \theta^-_{mn})} \tag{2.13}$$

$$Y_{mn}(\psi, \boldsymbol{k}) = -\frac{1}{2}\left[\sqrt{\frac{K_{00z}}{K_{mnz}}} + \sqrt{\frac{K_{mnz}}{K_{00z}}}\right]\cos\frac{\theta^+_{00} - \theta^-_{mn}}{2} + h_0 a_{3z}\sqrt{K_{00z}K_{mnz}}F^{(1)}_{00,mn}(\psi)\sin\frac{\theta^+_{00} - \theta^-_{mn}}{2} \tag{2.14}$$

and

$$F^{(1)}_{00,mn} = F_{00,mn} + \frac{\mathrm{i}}{2}(\beta_{00} + \beta_{mn}). \tag{2.15}$$

Using for $\mathrm{e}^{\mathrm{i}\psi^+_{00}}$ the value obtained from (2.12), after easy but lengthy algebraic manipulations, from (2.2) and (2.9), we get

$$\mathcal{R}_1(\boldsymbol{K}^-_{pq}) = \frac{k_z}{K_{pqz}}\left|\frac{\sqrt{\beta_{00}\beta_{mn}}\left[Y_{mn}(\psi^+_{00}, \boldsymbol{k}) \mp \sqrt{Y^2_{mn}(\psi^+_{00}, \boldsymbol{k}) - 1}\right]\sin\mathcal{X} + \beta_{00}\sin\mathcal{Y}}{2F^{(1)}_{00,mn}(\psi^+_{00})\sin\mathcal{Y}\sin\mathcal{X} + \beta_{00}\sin\mathcal{Y}\cos\mathcal{X} + \beta_{mn}\cos\mathcal{Y}\sin\mathcal{X}}\right|^2 \tag{2.16}$$

where

$$\mathcal{X} = \frac{\Gamma^-_{pq}}{2} \qquad \mathcal{Y} = \frac{\theta^-_{pq} - \theta^-_{mn}}{2}$$

and where $Y \mp \sqrt{Y^2-1} = Y - \mathrm{sgn}(Y)\sqrt{Y^2-1}$. Using formula (2.16) we can study the influence of the total reflection in one direction $\boldsymbol{K}^-_{mn}$ (e.g. $\boldsymbol{K}^-_{-10}$ in figure 2) on the reflectivity profile in another direction $\boldsymbol{K}^-_{pq}$ (e.g. $(-1-1)$). Putting $(mn) = (pq)$ in (2.16) we get the formula

$$\mathcal{R}_1(\boldsymbol{K}^-_{pq}) = \left[Y_{pq}(\psi^+_{00}, \boldsymbol{k}) \mp \sqrt{Y^2_{pq}(\psi^+_{00}, \boldsymbol{k}) - 1}\right]^2 \tag{2.17}$$

which has already been studied; see equation (3.3) in [1].

3. The influence of the Bragg reflections on the crystal truncation rod scattering

The formulae (2.16) and (2.17) for the evaluation of the reflectivity $\mathcal{R}_1(\boldsymbol{K}^-_{pq})$ in the direction $\boldsymbol{K}^-_{pq}$ are exact the choice of θ^-_{mn} in (2.16) being arbitrary. They of course contain the term $F^{(1)}_{00,mn}(\psi^+_{00})$ (see (2.14)) depending on the solution of the dispersion relation (2.10).

The advantage of formulae (2.14), (2.16) and (2.17) consists in the properties of the function $F^{(1)}_{00,mn}(\psi)$ given in (2.26*a*)–(2.26*d*) in [1], i.e.

$$F^{(1)}_{00,mn}(\psi) = 1 + \phi_{00,mn}(\psi) \tag{3.1}$$

the function $\phi_{00,mn}(\psi)$ having poles for (see (1.7) and the right-hand side of (2.10))

$$\psi = \begin{cases} \theta^+_{uv}(\boldsymbol{k}) & \text{except for } (uv) = (00) \\ \theta^-_{uv}(\boldsymbol{k}) & \text{except for } (uv) = (mn). \end{cases} \tag{3.2}$$

Outside these poles,

$$\phi_{00,mn}(\psi) = \mathrm{O}(1/h_0). \tag{3.3}$$

Thus, outside the poles (3.2) of the function $F^{(1)}_{00,mn}(\psi)$, equation (2.14) yields

$$Y_{mn}(\psi, \boldsymbol{k}) = Y_{mn}(\boldsymbol{k})\,[1 + \mathrm{O}(1/h_0)] \tag{3.4}$$

where

$$Y_{mn}(\boldsymbol{k}) = -\frac{1}{2}\left[\sqrt{\frac{K_{00z}}{K_{mnz}}} + \sqrt{\frac{K_{mnz}}{K_{00z}}}\right]\cos\frac{\theta^+_{00} - \theta^-_{mn}}{2} + h_0 a_{3z}\sqrt{K_{00z}K_{mnz}}\,\sin\frac{\theta^+_{00} - \theta^-_{mn}}{2}. \tag{3.5}$$

Let us note that the $Y_{mn}(\boldsymbol{k})$ only depends on the given 'geometrical parameters' $\boldsymbol{K}_{00}(\boldsymbol{k})$, $\boldsymbol{K}_{mn}(\boldsymbol{k})$, $\theta^+_{00}(\boldsymbol{k})$, $\theta^-_{mn}(\boldsymbol{k})$; it does not depend on the solutions of the dispersion relation (2.10).

Let us now consider (2.16) for the case where the incident wave is far from any Bragg or Laue diffraction position; thus $\theta^+_{00}(\boldsymbol{k})$ (see (1.4)) is far from any poles of the function $F^{(1)}_{00,mn}(\psi)$ (3.1) and the same holds due to (2.4) for ψ^+_{00}. Then

$$F^{(1)}_{00,mn}(\psi^+_{00}) = 1 + \mathrm{O}(1/h_0) \qquad Y_{mn}(\psi^+_{00}, \boldsymbol{k}) \mp \sqrt{Y^2_{mn}(\psi^+_{00}, \boldsymbol{k}) - 1} = \mathrm{O}(1/h_0) \tag{3.6}$$

and (2.16) reads

$$\begin{aligned}\mathcal{R}_1(\boldsymbol{K}^-_{pq}) &= \left|\frac{\beta_{00}\sin((\theta^-_{pq} - \theta^-_{mn})/2) + \mathrm{O}(1/h_0^2)}{2\sin((\theta^-_{pq} - \theta^-_{mn})/2)\sin(\Gamma^-_{pq}/2) + \mathrm{O}(1/h_0)}\right|^2 \frac{k_z}{K_{pqz}} \\ &= \frac{1 + \mathrm{O}(1/h_0)}{4h_0^2 a_{3z}^2 K_{00z} K_{pqz}\sin^2(\Gamma^-_{pq}/2)}.\end{aligned} \tag{3.7}$$

To show the influence of the Bragg diffraction positions, i.e. of the poles θ^-_{mn}, on the neutron scattering, let us apply formula (2.16) to say the non-coplanar reflection along CTR $(pq) = (-1\,-1)$, i.e. in the direction of the vector $\boldsymbol{K}^-_{-1-1}$; see the profile of Γ^-_{-1-1} in figure 2.

To avoid the poles of the functions $Y_{mn}(\psi_{00}^{+}, \boldsymbol{k})$ and $F^{(1)}_{00,mn}(\psi_{00}^{+})$, we shall use the same $(pq) = (-1\,-1)$ and different (mn) in (2.16). In the following we shall study two cases. In case A we shall obtain a formula for $\mathcal{R}_1(\boldsymbol{K}^{-}_{-1-1})$ valid only outside the regions of the angles of incidence $\gamma^{\mathrm{B}}_{001}$, $\gamma^{\mathrm{B}}_{-101}$ and $\gamma^{\mathrm{B}}_{000}$. A formula valid around the angle of incidence $\gamma^{\mathrm{B}}_{-101}$ is considered in case B.

3.1. Case A. $(mn) = (pq) = (-1, -1)$

In this case we use the exact formula for the reflectivity (2.17):

$$\mathcal{R}_1(\boldsymbol{K}^{-}_{-1-1}) = \left| Y_{-1-1}(\psi^{+}_{00}, \boldsymbol{k}) \mp \sqrt{Y^2_{-1-1}(\psi^{+}_{00}, \boldsymbol{k}) - 1} \right|^2. \tag{3.8}$$

However, the approximation (3.5) for $Y_{-1-1}(\psi^{+}_{00}, \boldsymbol{k})$ is justified only if the solution $\psi^{+}_{00} \doteq \theta^{+}_{00}$ lies outside the poles of the function $F^{(1)}_{00,-1-1}(\psi)$, i.e. if $\theta^{+}_{00}(\boldsymbol{k})$ is far (modulo 2π) from the poles

$$\theta^{+}_{uv}(\boldsymbol{k}),\ (uv) \neq (00) \qquad \text{and} \qquad \theta^{-}_{uv}(\boldsymbol{k}),\ (uv) \neq (-1, -1). \tag{3.9}$$

In other words we must avoid the angles of incidence γ where the conditions for any Laue or Bragg diffraction different from the direction $\boldsymbol{K}^{-}_{-1-1}$ are satisfied. Under these limitations we can write

$$\mathcal{R}_1(\boldsymbol{K}^{-}_{-1-1}) = \left| Y_{-1-1}(\boldsymbol{k}) \mp \sqrt{Y^2_{-1-1}(\boldsymbol{k}) - 1} \right|^2 [1 + \mathrm{O}(1/h_0)]. \tag{3.10}$$

The plot of (3.10) is given in figure 3. A plateau of the total reflection appears near $\gamma^{\mathrm{B1}}_{-1-12}$ and $\gamma^{\mathrm{B2}}_{-1-12}$, where $Y^2_{-1-1}(\boldsymbol{k}) < 1$. The regions of the total reflection were discussed in [1, 16, 17]. Far from these regions the second term on the right-hand side of (3.5) is very large and, similar to (3.7), we obtain

$$\mathcal{R}_1(\boldsymbol{K}^{-}_{-1-1}) = \frac{1 + \mathrm{O}(1/h_0)}{4h_0^2 a^2_{3z} K_{00z} K_{-1-1z} \sin^2(\Gamma^{-}_{-1-1}/2)}. \tag{3.11}$$

We eliminate the cases $K_{00z} = 0$ and $K_{-1-1z} = 0$ when the incident or reflected beams lie too close to the surface.

The approximation (3.10) does not hold close to $\gamma^{\mathrm{B}}_{001}$, $\gamma^{\mathrm{B}}_{-101}$ and $\gamma^{\mathrm{B}}_{000}$ (see figure 3), where the case B formulae have to be used instead.

Pinsker [3], p 267, gives for the reflection coefficient of a semi-infinite crystal a formula similar to our equation (2.17):

$$\mathcal{R}_{\mathrm{B}} = \left| \frac{\chi_h}{\chi_{-h}} \right| \left| y \pm \sqrt{y^2 - 1} \right|^2 \tag{3.12}$$

where the quantity y differs from our Y_{mn} (2.14). Formula (3.12) is valid only for the coplanar diffraction near the Bragg peak whereas (2.17) is valid for both coplanar and non-coplanar reflections and for any angle of incidence. A more detailed discussion can be found in [1].

3.2. Case B. $(pq) = (-1, -1)$ *and* $(mn) = (-10)$

Let us now consider the reflectivity $\mathcal{R}_1(\boldsymbol{K}^{-}_{-1-1})$ in the neighbourhood of the angle of incidence $\gamma^{\mathrm{B}}_{-101}$ where the condition for the Bragg reflection in the direction $\boldsymbol{K}^{-}_{-10}$ is satisfied (see figure 2), i.e. where

$$\theta^{+}_{00}(\boldsymbol{k}) = \theta^{-}_{-10}(\boldsymbol{k}) + 2\pi\ell + \eta_{-101}(\boldsymbol{k}) \qquad |\eta_{-101}(\boldsymbol{k})| \ll 1. \tag{3.13}$$

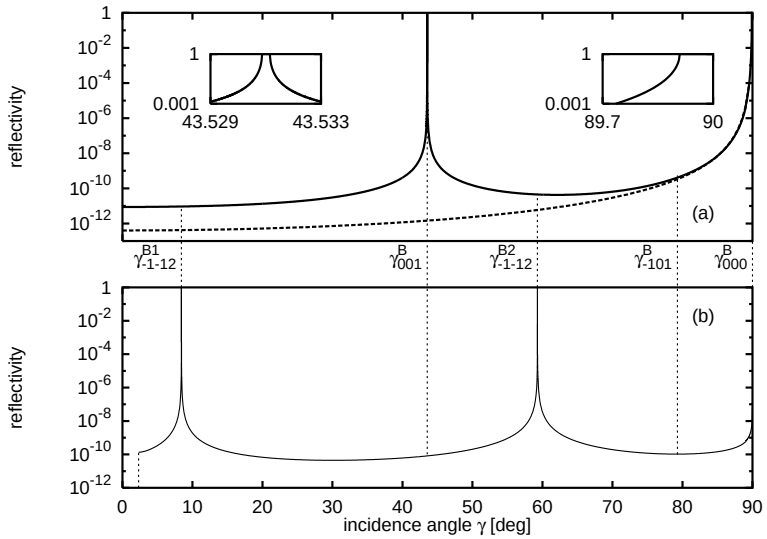

Figure 3. The reflectivities for the same parameters as in figure 1 in the approximation $F^{(1)}_{00,mn}(\psi^+_{00}) = 1$. The top graph shows the specular reflection $\mathcal{R}_1(\boldsymbol{K}^-_{00}) = |Y_{00}(\boldsymbol{k}) \mp \sqrt{Y^2_{00}(\boldsymbol{k}) - 1}|^2$, the bottom graph plots the non-coplanar reflection $\mathcal{R}_1(\boldsymbol{K}^-_{-1-1}) = |Y_{-1-1}(\boldsymbol{k}) \mp \sqrt{Y^2_{-1-1}(\boldsymbol{k}) - 1}|^2$; see equation (3.10). Vertical dotted lines near $\gamma^{\mathrm{B}}_{pq\ell}$ indicate the regions of γ where this approximation is not valid. In the scale of the figure the plots cannot be distinguished from the kinematical approximations $\mathcal{R}^{\mathrm{kin}}(\boldsymbol{K}^-_{pq}) = [4h_0^2 a^2_{3z} K_{00z} K_{pqz} \sin^2(\Gamma^-_{pq}/2)]^{-1}$, equation (4.3). The dotted curve in the upper graph is the reflectivity $\mathcal{R}^{\mathrm{geom}}(\boldsymbol{K}^-_{00}) = [2h_0 a^2_{3z} k^2_z]^{-2}$ using the classical Fresnel formulae (4.8). The inset figures show the plateaus of the total reflection at the Bragg diffraction position $\gamma^{\mathrm{B}}_{001}$ and total external reflection $\gamma^{\mathrm{B}}_{000}$.

In this case, ψ^+_{00} is near θ^-_{-10} and the approximation for $F^{(1)}_{00,-1-1}(\psi^+_{00}) = 1 + \mathrm{O}(1/h_0)$ used in the derivation of (3.10) does not hold. In this case, to avoid the pole θ^-_{-10} near ψ^+_{00}, we use in (2.16) $(mn) = (-10)$.

By choosing $(pq) = (-1, -1)$ and $(mn) = (-10)$ we get

$$\mathcal{R}_1(\boldsymbol{K}^-_{-1-1}) = \frac{k_z}{K_{-1-1z}} \left| \frac{\sqrt{\beta_{00}\beta_{-10}}\left[Y_{-10}(\psi^+_{00}, \boldsymbol{k}) \mp \sqrt{Y^2_{-10}(\psi^+_{00}, \boldsymbol{k}) - 1}\right] \sin \mathcal{W} + \beta_{00} \sin \mathcal{Z}}{2F^{(1)}_{00,-10}(\psi^+_{00}) \sin \mathcal{Z} \sin \mathcal{W} + \mathrm{O}(1/h_0)} \right|^2 \tag{3.14}$$

where

$$\mathcal{W} = \frac{\Gamma^-_{-1-1}}{2} \qquad \mathcal{Z} = \frac{\theta^-_{-1-1} - \theta^-_{-10}}{2}$$

For the evaluation of $Y_{-10}(\psi^+_{00}, \boldsymbol{k})$ we need $F_{00,-10}(\psi^+_{00})$. As ψ^+_{00} is near θ^+_{00} and θ^-_{-10}, it lies outside the poles of $F_{00,-10}(\psi)$ and the approximation $F_{00,-10}(\psi^+_{00}) = 1 + \mathrm{O}(1/h_0)$ is again valid. We get

$$\mathcal{R}_1(\boldsymbol{K}^-_{-1-1}) = \left(\left| \sqrt{\frac{K_{00z}}{K_{-10z}}} \frac{Y_{-10}(\boldsymbol{k}) \mp \sqrt{Y^2_{-10}(\boldsymbol{k}) - 1}}{\sin \mathcal{Z}} + \frac{1}{\sin \mathcal{W}} \right|^2 \Big/ (4h_0^2 a^2_{3z} K_{-1-1z} K_{00z}) \right) \times [1 + \mathrm{O}(1/h_0)]. \tag{3.15}$$

Near $\gamma^{\mathrm{B}}_{-101}$, equation (3.13) holds; thus,

$$\sin\frac{\theta^-_{-1-1}-\theta^-_{-10}}{2}=(-1)^{\ell+1}\sin\frac{\theta^+_{00}-\theta^-_{-1-1}}{2}\left[1+\mathrm{O}\left(\eta_{-101}\operatorname{cotan}\frac{\theta^-_{00}-\theta^-_{-1-1}}{2}\right)\right]. \tag{3.16}$$

Thus, near $\gamma^{\mathrm{B}}_{-101}$, equation (3.15) reads (in our case $\ell=1$)

$$\mathcal{R}_1(\boldsymbol{K}^-_{-1-1})=\frac{\left|\sqrt{K_{00z}/K_{-10z}}\left[Y_{-10}(\boldsymbol{k})\mp\sqrt{Y^2_{-10}(\boldsymbol{k})-1}\right]+1\right|^2}{4h_0^2a_{3z}^2K_{00z}K_{-1-1z}\sin^2(\Gamma^-_{-1-1}/2)}[1+\mathrm{O}(1/h_0)]. \tag{3.17}$$

In the region of the total reflection near $\gamma^{\mathrm{B}}_{-101}$ it holds that $Y_{-10}(\boldsymbol{k})\in[-1,1]$, i.e. $\mathcal{R}_1(\boldsymbol{K}^-_{-1-1})$ has its values in the interval

$$\left|1\pm\sqrt{\frac{K_{00z}}{K_{-10z}}}\right|^2\frac{1+\mathrm{O}(1/h_0)}{4h_0^2a_{3z}^2K_{00z}K_{-1-1z}\sin^2(\Gamma^-_{-1-1}/2)}. \tag{3.18}$$

We can see that the influence of the total reflection in the direction $\boldsymbol{K}^-_{-10}$ on the reflectivity $\mathcal{R}_1(\boldsymbol{K}^-_{-1-1})$ is near the angle $\gamma^{\mathrm{B}}_{-101}$ considerable. But far from this region, the term

$$Y_{-10}(\boldsymbol{k})\pm\sqrt{Y^2_{-10}(\boldsymbol{k})-1}$$

in (3.17) is of the order of $1/h_0$. Thus, far from $\gamma^{\mathrm{B}}_{-101}$ it holds that

$$\mathcal{R}_1(\boldsymbol{K}^-_{-1-1})=\frac{1+\mathrm{O}(1/h_0)}{4h_0^2a_{3z}^2K_{00z}K_{-1-1z}\sin^2(\Gamma^-_{-1-1}/2)} \tag{3.19}$$

which is the same limit as in (3.7) and (3.11). By applying this restriction we exclude again the cases where $K_{00z}=0$ and $K_{-1-1z}=0$ (the beginning and end of the reflection plot $\boldsymbol{K}^-_{-1-10}$).

The reflectivity $\mathcal{R}_1(\boldsymbol{K}^-_{-1-1})$ near $\gamma^{\mathrm{B}}_{001}$—see figure 4(b)—and the specular reflectivity $\mathcal{R}_1(\boldsymbol{K}^-_{00})$ near $\gamma^{\mathrm{B1}}_{-1-12}$, $\gamma^{\mathrm{B2}}_{-1-12}$ and $\gamma^{\mathrm{B}}_{-101}$, can be studied in the same way.

Generally, near the Bragg angle $\gamma^{\mathrm{B}}_{mn\ell}$, where the Bragg diffraction condition in the direction $\boldsymbol{K}^-_{mn}\neq\boldsymbol{K}^-_{pq}$ is satisfied, we get from (2.16)

$$\mathcal{R}_1(\boldsymbol{K}^-_{pq})=\frac{\left|(-1)^{\ell+1}\sqrt{K_{00z}/K_{mnz}}\left[Y_{mn}(\boldsymbol{k})\mp\sqrt{Y^2_{mn}(\boldsymbol{k})-1}\right]+1\right|^2}{4h_0^2a_{3z}^2K_{00z}K_{pqz}\sin^2(\Gamma^-_{pq}/2)}[1+\mathrm{O}(1/h_0)]. \tag{3.20}$$

In figure 4(b) we plot the non-coplanar reflectivity $\mathcal{R}_1(\boldsymbol{K}^-_{-1-1})$ near the angle of the total reflection $\gamma^{\mathrm{B}}_{001}$ for the specular reflection, using formula (3.20) for $(pq)=(-1\,-1)$, $(mn)=(00)$, $\ell=1$ (full curve) and the approximation (3.10) (dashed curve).

So far we have studied the influence of the poles θ^-_{rs} of the dispersion relation (1.7) on the reflectivity of a semi-infinite crystal. Let us now assume that $\theta^+_{00}(\boldsymbol{k})$ is near a pole $\theta^+_{rs}(\boldsymbol{k})$ (mod 2π), i.e. that the incident wave vector $\boldsymbol{k}$ approximately satisfies the condition (1.6) for the Laue diffraction into the direction $\boldsymbol{K}^+_{rs}(\boldsymbol{k})$. Analysing this case by a method similar to the case shown above we would come to the result that the Laue diffraction position does not influence the reflectivity $\mathcal{R}_1(\boldsymbol{K}^-_{-1-1})$ given by formula (3.10).

4. Comparison with the kinematical theory and geometrical optics approximations

Let us now compare our results based on Ewald's dynamical theory of diffraction with the *kinematical theory*. In the kinematical approximation, the wave function for the reflection by a crystalline slab of the thickness N_3a_{3z} reads (compare with (2.1*a*), (2.1*b*) in [1])

$$\Psi(\boldsymbol{r})=A\mathrm{e}^{\mathrm{i}\boldsymbol{k}\cdot\boldsymbol{r}}-A\sum_{n_3=0}^{N_3}\sum_{n_1,n_2=-\infty}^{+\infty}Q\frac{\mathrm{e}^{\mathrm{i}k\cdot|\boldsymbol{r}-\boldsymbol{R}_n|}}{|\boldsymbol{r}-\boldsymbol{R}_n|}\mathrm{e}^{\mathrm{i}\boldsymbol{k}\cdot\boldsymbol{R}_n}. \tag{4.1}$$

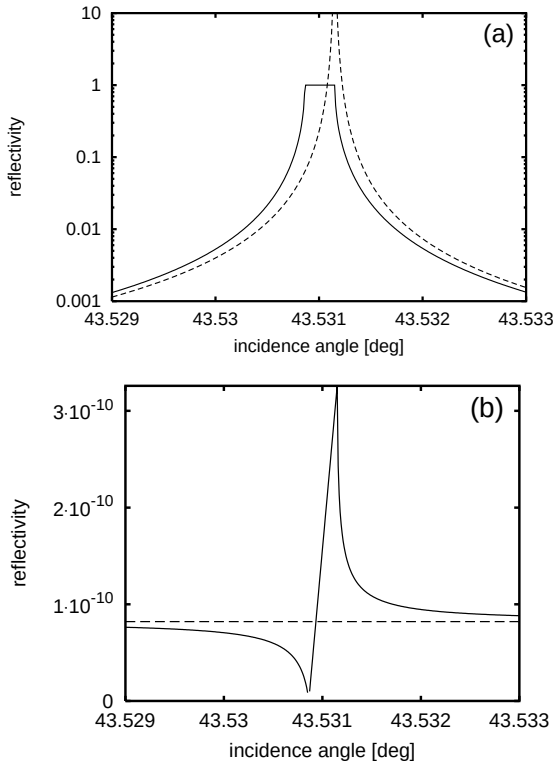

Figure 4. The plots of the reflectivities near $\gamma^{\mathrm{B}}_{001}$. (a) The specular reflectivity $\mathcal{R}_1(\boldsymbol{K}^-_{00})$. Full curve: $\mathcal{R}_1(\boldsymbol{K}^-_{00}) = |Y_{00}(\boldsymbol{k}) \mp \sqrt{Y^2_{00}(\boldsymbol{k}) - 1}|^2$; equation (5.1). Dashed curve: $\mathcal{R}^{\mathrm{kin}}(\boldsymbol{K}^-_{00}) = [4h_0^2 a_{3z}^2 k_z^2 \sin^2(a_{3z}k_z)]^{-1}$, equation (4.4). (b) The non-coplanar reflectivity $\mathcal{R}_1(\boldsymbol{K}^-_{-1-1})$. Full curve: $\mathcal{R}_1(\boldsymbol{K}^-_{-1-1}) = |Y_{00}(\boldsymbol{k}) \mp \sqrt{Y^2_{00}(\boldsymbol{k}) - 1} + 1|^2/[4h_0^2 a_{3z}^2 K_{00z} K_{-1-1z} \sin^2(\Gamma^-_{-1-1}/2)]$; equation (3.20) for $(pq) = (-1\,-1)$, $(mn) = (00)$, $\ell = 1$. Dashed curve: the approximation $\mathcal{R}_1(\boldsymbol{K}^-_{-1-1}) = |Y_{-1-1}(\boldsymbol{k}) \mp \sqrt{Y^2_{-1-1}(\boldsymbol{k}) - 1}|^2$; equation (3.10).

Using the formula derived in [15] for the plane sum over (n_1, n_2) we get

$$\Psi(\boldsymbol{r}) = A\mathrm{e}^{\mathrm{i}\boldsymbol{k}\cdot\boldsymbol{r}} + A\frac{2\pi\, Q\mathrm{i}a_{3z}}{|\boldsymbol{a}_1 \times \boldsymbol{a}_2|}\sum_{uv}\frac{\mathrm{e}^{\mathrm{i}\theta^-_{uv}}}{a_{3z}K_{uvz}}\frac{1 - \mathrm{e}^{\mathrm{i}(N_3+1)(\boldsymbol{k}\cdot\boldsymbol{a}_3 - \theta^-_{uv})}}{\mathrm{e}^{\mathrm{i}\theta^+_{00}} - \mathrm{e}^{\mathrm{i}\theta^-_{uv}}}\mathrm{e}^{\mathrm{i}\boldsymbol{K}^-_{uv}\cdot\boldsymbol{r}}. \tag{4.2}$$

The transition from a thick crystal to a semi-infinite one can be performed by introducing a small absorption. Then the wave vector in the crystal has a small imaginary part which smooths the rapidly oscillating term in (4.2) and we get

$$\mathcal{R}^{\mathrm{kin}}(\boldsymbol{K}^-_{pq}) = \frac{1}{4h_0^2 a_{3z}^2 K_{00z} K_{pqz} \sin^2(\Gamma^-_{pq}/2)} \tag{4.3}$$

where $Q \approx Q_0$ was used. The specular reflectivity is given explicitly by

$$\mathcal{R}^{\mathrm{kin}}(\boldsymbol{K}^-_{00}) = \frac{1}{4h_0^2 a_{3z}^2 k_z^2 \sin^2 a_{3z}k_z} \tag{4.4}$$

and it is plotted in figure 3. Comparing (4.3) with (3.7), (3.11) and (3.19), we can conclude

that, in the regions far from any Bragg peaks, the kinematical theory of diffraction yields results which are very close to the dynamical theory of diffraction.

In the *geometrical optics* approximation, the slab is considered as a homogeneous medium. The optical potential, representing the effective interaction of the neutron with the medium, is [4]

$$V_0 = \frac{\overline{h}^2}{m a_{3z}^2} \frac{1}{h_0} \tag{4.5}$$

where m is the mass of the neutron. There is only one wave that is reflected and only one wave that is refracted. For the z-component of the refracted wave,

$$\kappa_z^0 = \sqrt{k_z^2 - \frac{2}{a_{3z}^2 h_0}} \tag{4.6}$$

holds. This represents the classical Snell law. The coefficient of reflection is the well-known Fresnel coefficient of classical optics:

$$\zeta_0 = \frac{k_z - \kappa_z^0}{k_z + \kappa_z^0} = \frac{1 + \mathrm{O}(1/h_0)}{2h_0 (a_{3z} k_z)^2}. \tag{4.7}$$

Thus for the reflectivity of the specularly reflected beam we get (see figure 3)

$$\mathcal{R}^{\mathrm{geom}}(\boldsymbol{K}_{00}^-) = \zeta_0^2 = \frac{1 + \mathrm{O}(1/h_0)}{4h_0^2 a_{3z}^4 k_z^4}. \tag{4.8}$$

We can compare the kinematical (4.4) and geometrical optics (4.8) formulae by evaluating their ratio

$$\frac{\mathcal{R}^{\mathrm{kin}}(\boldsymbol{K}_{00}^-)}{\mathcal{R}^{\mathrm{geom}}(\boldsymbol{K}_{00}^-)} = \left[\frac{a_{3z} k_z}{\sin(a_{3z} k_z)}\right]^2 [1 + \mathrm{O}(1/h_0)]. \tag{4.9}$$

This is the well-known formula appearing in the study of the soft x-ray reflection [18, 19]. The plots of this ratio for several wavelengths, figure 5, demonstrate the limited validity of the Fresnel formulae for the truncation rod scattering when the wavelength is comparable to the lattice parameter.

5. Conclusions

We have studied the reflectivity of neutrons incident on an ideal semi-infinite crystal within Ewald's multiwave dynamical theory of diffraction. To summarize, we can say that the exact expression for the reflectivity $\mathcal{R}(\boldsymbol{K}_{pq}^-)$ along a crystal truncation rod (pq), equation (2.1), is given by formulae (2.8), (2.9), (2.16) and (2.17), where the $Y_{mn}(\psi)$ in these formulae are given by (2.14). These expressions are exact, but to use them we need the solution ψ_{00}^+ of the dispersion equation (1.7). Thus several approximations have been derived, which eliminate the need for evaluating ψ_{00}^+.

Firstly, outside the regions close to the Bragg angles $\gamma_{mn\ell}^{\mathrm{B}}$, $(mn) \neq (pq)$, it holds that (see equation (3.10))

$$\mathcal{R}_1(\boldsymbol{K}_{pq}^-) = \left| Y_{pq}(\boldsymbol{k}) \mp \sqrt{Y_{pq}^2(\boldsymbol{k}) - 1} \right|^2 [1 + \mathrm{O}(1/h_0)] \tag{5.1}$$

where the function $Y_{pq}(\boldsymbol{k})$, equation (3.5), is independent of ψ_{00}^+.

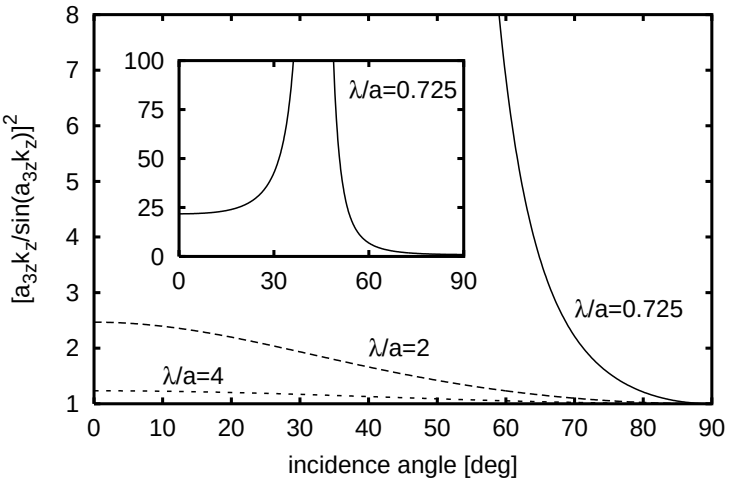

Figure 5. The ratio $\mathcal{R}^{\mathrm{kin}}(\boldsymbol{K}^-_{00})/\mathcal{R}^{\mathrm{geom}}(\boldsymbol{K}^-_{00}) = [a_{3z}k_z/\sin(a_{3z}k_z)]^2$, where $a_{3z}k_z = (\pi a/\lambda)\cos\gamma$ (see equation (4.9)), for several wavelengths. The Fresnel formulae can be applied in regions where the ratio is close to 1 for a given λ/a.

Secondly, near the Bragg angle $\gamma^{\mathrm{B}}_{mn\ell}$, where the Bragg diffraction in the direction of $\boldsymbol{K}^-_{mn} \neq \boldsymbol{K}^-_{pq}$ appears, the approximation (5.1) should be replaced by (see (3.20))

$$\mathcal{R}_1(\boldsymbol{K}^-_{pq}) = \frac{\left|(-1)^{\ell+1}\sqrt{K_{00z}/K_{mnz}}\left[Y_{mn}(\boldsymbol{k}) \mp \sqrt{Y^2_{mn}(\boldsymbol{k})-1}\right]+1\right|^2}{4h_0^2 a_{3z}^2 K_{00z} K_{pqz}\sin^2(\Gamma^-_{pq}/2)}[1+\mathrm{O}(1/h_0)]. \tag{5.2}$$

Outside the regions of the Bragg diffraction positions $\gamma^{\mathrm{B}}_{uv\ell}$ in any direction $\boldsymbol{K}^-_{uv}$, both formulae (5.1), (5.2) converge to (3.7):

$$\mathcal{R}_1(\boldsymbol{K}^-_{pq}) = \frac{1+\mathrm{O}(1/h_0)}{4h_0^2 a_{3z}^2 K_{00z} K_{pqz}\sin^2(\Gamma^-_{pq}/2)}. \tag{5.3}$$

Formula (5.3) agrees very well with the kinematical formula (4.3).

In the approximation of the geometrical optics the crystal is considered as a homogeneous medium characterized by the optical potential (4.5). The reflectivity for the specular reflection is given by $\mathcal{R}^{\mathrm{geom}}(\boldsymbol{K}^-_{00})$, equation (4.8). For the ratio $\mathcal{R}^{\mathrm{kin}}(\boldsymbol{K}^-_{00})/\mathcal{R}^{\mathrm{geom}}(\boldsymbol{K}^-_{00})$ a simple relation (4.9) holds.

In figure 3 we show the plots of the reflectivities $\mathcal{R}_1(\boldsymbol{K}^-_{00})$ and $\mathcal{R}_1(\boldsymbol{K}^-_{-1-1})$ in the approximation (5.1). In figure 4(a) we give the detail of $\mathcal{R}_1(\boldsymbol{K}^-_{00})$, equation (5.1), in the region of the total reflection together with the kinematical approximation (5.3). In figure 4(b) we show the influence of the total reflection in the direction $\boldsymbol{K}^-_{00}$ around the Bragg angle $\gamma^{\mathrm{B}}_{001}$ on the reflectivity $\mathcal{R}_1(\boldsymbol{K}^-_{-1-1})$ by applying (5.2) with $(pq) = (-1\,-1)$ and $(mn) = (00)$. The approximation (5.1) in this region is also demonstrated. Figure 5 demonstrates a simple relationship between the kinematical theory and geometrical optics approximation for several wavelengths.

Special attention should be paid to the regions where our formulae diverge—that is, to the regions close to the start and end points of the reflection curve for $\boldsymbol{K}^-_{pq}$.

The approach presented here could be used to analyse the analytical approximate formulae for the case where three (or more) poles of the dispersion relation (1.7) coincide, i.e. when the

Ewald sphere intersects three (or more) nodes of the three-dimensional reciprocal lattice. In this case it would be necessary to shift the appropriate poles from right to left in (2.10).

Finally, let us note that the truncation rod scattering was studied in [11] using the Darwin procedure. It can be shown that formula (2.25) in [11] comports with our results. An application to the coplanar three-beam case leads in [11] to a cubic equation; thus analytical comparison with our results seems to be very difficult. But the plot of the reflectivity in figure 9 in [11] seems to be very similar to our figure 4(b) based on formulae (5.2).

Acknowledgments

We thank Professors M Lenc and V Holý for critically reading the manuscript. The work of PM was supported by the grant VS 96102 of the Ministry of Education of the Czech Republic.

References

[1] Litzman O, Mikulík P and Dub P 1996 *J. Phys.: Condens. Matter* **8** 4709
[2] Zachariasen W H 1946 *Theory of X-ray Diffraction in Crystals* (New York: Wiley)
[3] Pinsker Z G 1978 *Dynamical Scattering of X-Rays in Crystals* (Berlin: Springer)
[4] Sears V F 1989 *Neutron Optics* (Oxford: Oxford University Press)
[5] Andrews R S and Cowley R A 1985 *J. Phys. C: Solid State Phys.* **18** 6427
[6] Robinson I K 1986 *Phys. Rev.* B **33** 3830
[7] Usta K A, Dosch H and Peisl J 1990 *Z. Phys.* B **79** 404
[8] Colella R 1991 *Phys. Rev.* B **43** 13 827
[9] Caticha A 1993 *Phys. Rev.* B **47** 76
[10] Caticha A 1994 *Phys. Rev.* B **49** 33
[11] Takahashi T and Nakatani S 1995 *Surf. Sci.* **326** 347
[12] Ewald P P 1916 *Ann. Phys., Lpz.* **49** 1
Ewald P P 1917 *Ann. Phys., Lpz.* **54** 519
Ewald P P 1932 *Ann. Inst. H Poincaré* II **8** 79
[13] Litzman O 1978 *Opt. Acta* **25** 509
Litzman O 1980 *Opt. Acta* **27** 231
[14] Dederichs P H 1972 *Solid State Physics* vol 27, ed H Ehrenreich, F Seitz and D Turnbull (New York: Academic)
[15] Litzman O 1986 *Acta Crystallogr.* A **42** 552
[16] Dub P, Litzman O and Mikulík P 1996 *Scr. Fac. Sci. Univ. Masarykianae Brunensis (Physica)* **24–26** 5
[17] Litzman O and Dub P 1990 *Acta Crystallogr.* A **46** 247
[18] Litzman O and Rózsa P 1984 *Opt. Acta* **31** 1351
[19] Litzman O and Šebelová I 1985 *Opt. Acta* **32** 839